Mechanical Technology and Engineering Insights

www.mtei.reapress.com

Mech. Technol. Eng. Insights . Vol. 1, No. 2 (2024) 122–131.

Paper Type: Original Article

A Geometrically Self Compensated MEMS Capacitive Pressure Sensor with High Thermal Stability

Mojtaba Malekee[1,*], Mohammadreza Kazempoor[2]

[1] Department of Mechanical Engineering, Faculty of Mechanical Engineering, University of Guilan, Rasht, Guilan, Iran; mojtaba.malekee@gmail.com.

[2] Department of Mechanical Engineering, Islamic Azad University, Siahkal Center, Siahkal, Guilan, Iran; mkazempur@gmail.com.

Citation:

Received: 16 Frbruary 2024 *Revised: 18 April 2024* *Accepted:18 June 2024*	Malekee, M., & Kazempoor, M. (2024). A geometrically self compensated MEMS capacitive pressure sensor with high thermal stability. *Mechanical Technology and Engineering Insights, 1*(2), 122-131.

Abstract

This paper proposes a highly sensitive capacitive pressure sensor for which a new thermal-compensation method has been developed. The new method uses a geometric approach to compensate for the decrease in Young's modulus with temperature. The method is based on connecting a mass spring with a larger spring that is connected to the anchor. Because of the difference in thermal expansion of the large spring and the small spring, the smaller spring would experience axial tensile forces, leading to an increase in its stiffness. Thus, the increase in stiffness of the smaller spring could compensate for the decrease in the spring constant of the larger spring because of the thermal dependence of the Young's modulus. The pressure error due to temperature changes in the compensated sensor is less than 33 Pa, demonstrating a remarkable improvement compared with previous literature reports. The sensor's occupied area is about 0.03288 mm^2, and its sensitivity is 290 ppm. Compared with state-of-the-art Micro-Electro-Mechanical Systems (MEMS) capacitive pressure sensors reported in the literature between 2015 and 2024, the Temperature Coefficient of Sensitivity (TCS) obtained with the proposed design achieves an extremely low value of 28.52 ppm/°C.

Keywords: Capacitive pressure sensor, Micro-electro-mechanical systems, Thermal compensation, Temperature dependence, Young's modulus, Geometrical compensation.

1 | Introduction

Micro-Electro-Mechanical Systems (MEMS) pressure sensors have been applied in many industries, including automotive, aerospace, biomedical engineering, cell phone technology, and microphone applications. Another application includes fingerprint sensors [1], blood vessel pressure measurements [2], and cerebrospinal fluid pressure measurements [3]. These types of measurements require highly sensitive, temperature-insensitive

Corresponding Author: mojtaba.malekee@gmail.com

https://doi.org/10.48313/mtei.v1i2.53

pressure sensors; moreover, these sensors should be able to measure very low pressures. Among different measurement technologies, the capacitive measurement technique offers high accuracy, sensitivity, very low power consumption, and integration with electronics [4], [5]. The physical principle of capacitors is quite simple; however, it is very accurate in detecting displacements. This type of sensor usually uses one or more movable plates and one or more stationary plates. The basic capacitance equation is:

$$C = \frac{\varepsilon_o A}{d}. \quad (1)$$

Temperature affects all parameters in *Eq. (1)* and can introduce large measurement errors. If the material's temperature sensitivity is low, the change is small, and the resulting capacitance variations can be neglected. Additionally, due to the limited thermal expansion coefficient of silicon, this, effect is very small. The main problem is the temperature sensitivity of the material's Young's modulus. Due to much lower fabrication costs compared to other materials, excellent mechanical properties and stability, and compatibility with electronic circuits, polycrystalline silicon (polysilicon) is used as the structural material. Increased temperature reduces Young's modulus and decreases the spring constant of the diaphragm. This leads to larger diaphragm displacement for a fixed pressure at different temperatures, causing significant errors in capacitance measurement and consequently in the applied pressure reading. This paper proposes a new geometric solution to overcome this problem.

All of the factors in *Eq. (1)* depend on the temperature, and hence there can be substantial errors in measuring them. If the material's temperature dependence is low, the factor will be sufficiently low, and the error from capacitance variations will be negligible. Moreover, because silicon's coefficient of thermal expansion is relatively low, the effect is minimal. The biggest challenge here is the temperature dependence of Young's modulus. Since polysilicon is inexpensive, has excellent mechanical properties, and is compatible with electronic circuits, it is used as a structural material. An increase in temperature lowers Young's modulus and reduces the spring constant. Thus, the diaphragm displacement for the same pressure depends considerably on temperature, making it impossible to measure pressure accurately due to errors in capacitance.

Some work has been carried out on thermal compensation methods at both the material and structural levels in MEMS pressure sensors. Self-packaging of a capacitive absolute pressure sensor using MEMS technology for high-temperature applications without electrical compensation was reported by Ghanam et al. [6], resulting in thermal drift of less than –0.0005% FS/K at 220°C. A thermally stable MEMS shielded capacitive pressure sensor was fabricated using the TSV hermetic packaging method in [7]. For touch-mode capacitive pressure sensors, a concave well substrate structure [8] greatly enhanced sensor sensitivity by using a notched diaphragm. Analytical methods for square diaphragm capacitive pressure sensors were formulated by [9], with a lower computational cost than the FEM method. The performance of different diaphragm materials (polysilicon, silicon nitride, 3C SiC) in touch-mode MEMS pressure sensors at high temperatures has been investigated by [10], providing useful information for designing such sensors for the automotive industry. A silicon polysilicon square diaphragm sensor was studied in [11], with a sensitivity of 30×10^{-6} pF/Pa over 290-300 K. A biocompatible MEMS capacitive pressure sensor was designed in [12], demonstrating good linearity and sensitivity.

Recently, a neural network that operates within a sensor system for real-time thermal drift compensation has been introduced [13], [14]. This innovation has enabled errors as small as ±0.05 KPa with only 0.0373 mm² of space. These developments clearly indicate the increasing significance of mechanical and intelligent compensation approaches over complicated electronics.

In contrast to earlier research that relies on electronic circuits, reference capacitors, and post-fabrication calibration [6], [7], [13], [14] this paper introduces an innovative approach based entirely on geometric compensation. Through the use of differential thermal expansion of two springs, it is possible to overcome the effect of decreasing Young's modulus of elasticity due to increasing temperatures.

2 | Design of the Pressure Sensor with Thermal Compensation

The pressure sensor's design employs a geometric thermal compensation method. The following thermal effects affect the pressure sensor springs: an increase in temperature decreases the Young's modulus of polysilicon (see *Fig. 1*). As a result, the diaphragm spring constant decreases. Thus, there is an expansion in capacitance measurements under constant pressure and various temperatures. An increase in temperature also extends the beams in the longitudinal direction. *Fig. 2* shows the schematic diagram of the pressure sensor. Spring K is considerably wider than spring K', and therefore much stiffer. Hence, under pressure, spring K will have less deformation than K'. Thus, point A serves as a virtual support for spring K'.

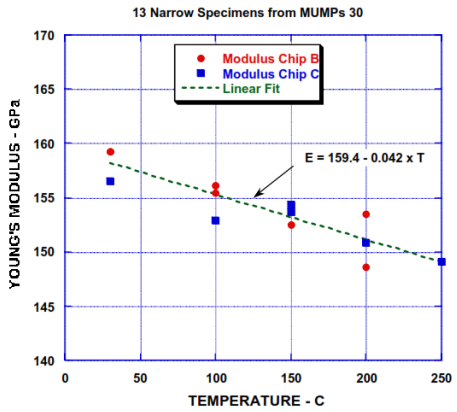

Fig. 1. Young's modulus vs. temperature for polysilicon [15].

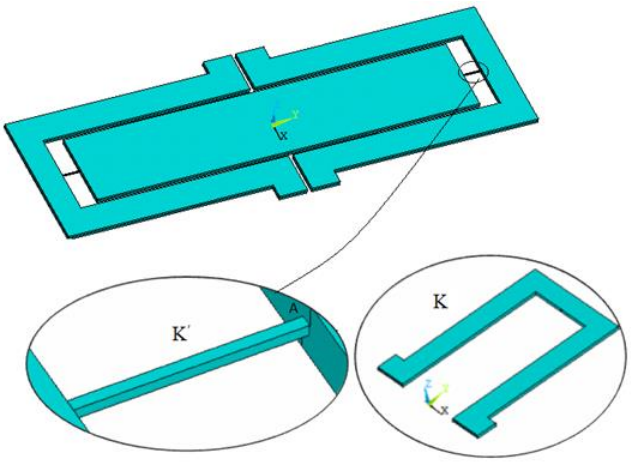

Fig. 2. Schematic of the proposed capacitive pressure sensor.

Thermal effect two involves the lengthening of the spring due to thermal expansion. The long spring K is thermally elongated more compared to the shorter spring K'. Thermal elongation results in tensile stresses in spring K' because of its lower thermal elongation. The other end of the spring K' is connected to the proof mass that cannot move.

The tensile stress in spring K' makes it harder to bend. The stiffened spring K' resists the downward bending of the diaphragm caused by applied pressure. The spring constants of springs K' and K can be determined from *Eqs. (2)* and *(3)*. The tensile stress in the small spring caused by the larger spring as a result of temperature change can be obtained from equation:

$$K' = \frac{1}{4} E w' \left(\frac{t'}{l'}\right)^3. \quad (1)$$

$$K = 4Ew\left(\frac{t}{l}\right)^3.$$

$$\Delta L_T = \Delta L - \Delta L' = \alpha \Delta T (L - L'),$$

where ΔL and ΔL' are the longitudinal expansions of springs K and K', ΔT is the temperature change, and ΔL_T is the tensile displacement induced in K'. E is Young's modulus, w', t', l', and w, t, l are the width, thickness, and length of the small and large springs, respectively, and α is the thermal expansion coefficient.. To model this tension, a force F is applied to spring K' to create an equivalent displacement ΔL_T (*Fig. 3*). This force is given by:

$$F = K' \Delta L_T.$$

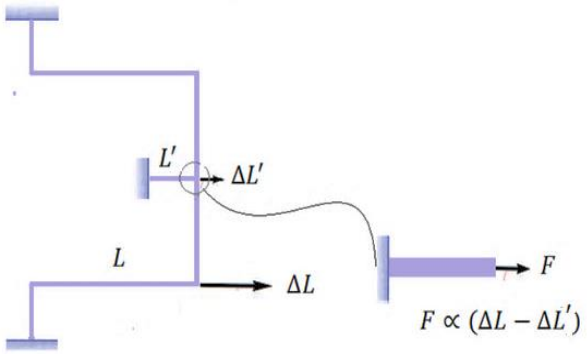

Fig. 3. Tensile force induced in the small spring due to differential thermal expansion between the large and small springs.

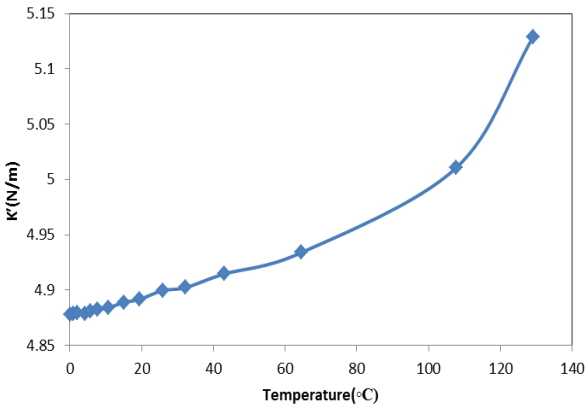

Fig. 4. Variation of spring stiffness K' with temperature.

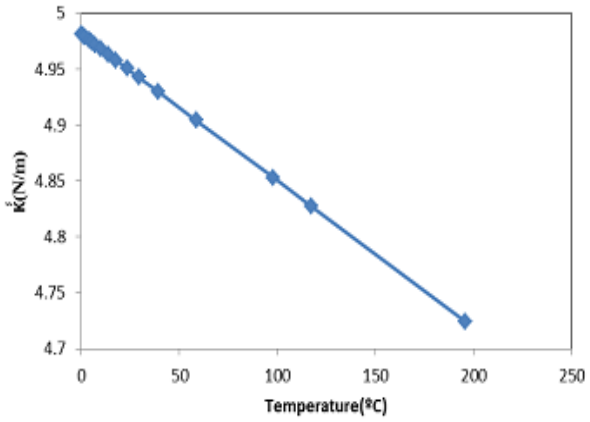

Fig. 5. Reduction of spring constant K'(T) due to temperature.

The frequency of the bending mode in the presence of prestress can be determined using ANSYS. The frequency is thus expressed as:

$$f = \frac{1}{2\pi}\sqrt{\frac{K'}{M'_{eff}}}, \tag{6}$$

where M'_eff is the effective mass of the spring K'. To obtain the thermal effect compensation, the spring length L should be larger than L'. Also, in order to satisfy that K >> K', L should be wider and thicker than L'. From *Fig. 1*, the approximate relation between E and temperature at operating temperatures can be expressed as:

$$E = 159.4 - 0.042T(GPa). \tag{7}$$

For convenience in the fabrication process, we set w' and t' to 1 μm, and w and t to 5 μm. Thus, K >> K'.

$$\Delta C = \varepsilon A\left(\frac{1}{d-\Delta d} - \frac{1}{d}\right). \tag{8}$$

Fig. 4 illustrates the change of K' with respect to ΔL_T as temperature changes, and *Fig. 5* shows the change in the value of K'(T) because of the decrease in Young's modulus during heating.

$$\Delta p = \frac{Ew'\left(\frac{t'}{l'}\right)^3 \Delta d}{2A}. \tag{9}$$

From the capacitance change with respect to pressure, sensor sensitivity can be derived as:

$$\frac{\Delta C}{\Delta p} = \frac{2\varepsilon A^2}{Ew'\left(\frac{t'}{l'}\right)^3 d(d-\Delta d)} \tag{10}$$

3 | Simulation Results

Fig. 6 shows the static structural analysis of the sensor under applied pressure on the main plate. As predicted, the displacement of the large spring is negligible compared to the small spring, validating the virtual anchor assumption. Displacement vector plots (*Fig. 7*) help understand the movement direction of each element. The plate displacement Δd under 100 Pa pressure is approximately 0.1597 μm.

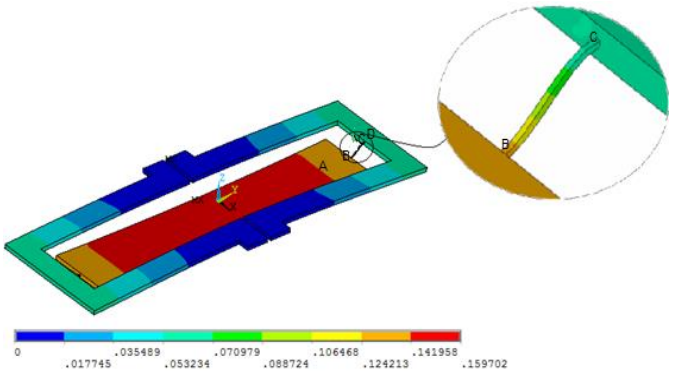

Fig. 6. Static structural analysis of the proposed pressure sensor under an applied pressure of 100 Pa – displacement contour plot.

For the sensor with spring K, at a reference temperature T_1 = 20°C and pressure 1000 Pa, displacement d_1 = 1.54 μm. At T_2 = 140°C under the same pressure, d_2 = 1.59 μm. The equivalent pressure at T_1 that produces the same displacement is 1032.46 Pa, giving a pressure error of 32.46 Pa. The temperature sensitivity of the sensor is 255 ppm.

Without spring K, at T_1 = 20°C and 1000 Pa, d_1 = 1.169 μm. At T_2 = 140°C, d_2 = 4.342 μm. The equivalent pressure error is 2714.28 Pa, with a temperature sensitivity of 22619.05 ppm. Thus, adding spring K dramatically reduces temperature sensitivity, achieving near-ideal In *Table 1* below, the changes in displacement and pressure errors of the sensor are presented for two temperatures (20 °C and 140 °C) at a constant applied pressure of 1000 Pa, both with and without the spring K.

For the case where the spring K is included: As the temperature increases from 20 °C to 140 °C, the displacement changes negligibly from 1.54 μm to 1.59 μm. As a result, there is an insignificant pressure error of just 32.46 Pa, which is 255 ppm in terms of relative error. This shows the efficiency of the geometrical compensation approach.

For the case without the inclusion of spring K: The displacement changes by a factor of 3.7 from 1.169 μm to 4.342 μm. With such displacement changes, the pressure error reaches 2714 Pa, which corresponds to 22619 ppm. The characteristics of the proposed compensated sensor are presented in *Table 2* below.

The proposed sensor has a wide pressure-sensing range of 50 Pa to 5000 Pa and an exceptionally wide temperature operating range of 0 °C to 260 °C. The Temperature Coefficient of Sensitivity (TCS) is 28.52 ppm/°C; one of the smallest that have been achieved with mechanical compensation alone. Capacitance to pressure sensitivity (ΔC/Δp) was 27.46 fF/kPa.

Table 3 compares the proposed design with 14 reported MEMS capacitive pressure sensors, including traditional sensors from the literature published between 2002 and 2013 and modern papers published between 2021 and 2023 in Elsevier and Springer.

Previous sensors generally have TCOs in the range of 30 ppm/°C to 180 ppm/°C, with some exceeding 1000 ppm/°C (when uncompensated). The two neural network-based compensation methods [19,20] perform excellently, with very low residual errors of ±0.5 hPa, but require active electronic components and consume energy. On the other hand, the present approach demonstrates an impressive TCO of 28.52 ppm/°C (the best value of any purely mechanical system), a high ΔC/Δp ratio of 27.46 fF/kPa, and consumes zero power for compensation. The uncompensated version of our device (Row 16) also possesses a significantly large TCO value of 7781 ppm/°C.

Table 1. Simulation results with and without spring K (at constant 1000 Pa).

Parameter	With Spring K	Without Spring K
Displacement at T_1=20°C	1.54 μm	1.169 μm
Displacement at T_2=140°C	1.59 μm	4.342 μm
Equivalent read pressure at 20°C	1032.46 Pa	3714.28 Pa
Pressure error	32.46 Pa	2714.28 Pa
Error (ppm)	255 ppm	22619.05 ppm

Table 2. Performance parameters of the proposed sensor.

Parameter	Value
Pressure range	50 – 5000 Pa
Temperature range	0 – 260 °C
Temperature sensitivity of sensor	28.52 ppm/°C
Capacitance change vs. pressure (ΔC/Δp)	27.46 fF/kPa

Table 3. Comparison with previous works (original and recent).

Reference	Temp. Range (°C)	TCO / Drift	ΔC/Δp (fF/kPa)
Matsumoto and Esasi [16]	20–140	100 ppm/°C	1.1
Ganji and Shahiri-Tabarestani [17]	25–100	170 ppm/°C	0.59
Hao et al. [18]	20–50	111 ppm/°C	2.29
Eswaran and Malarvizhi [19]	70–150	30.98 ppm/°C	20
Fang et al. [20]	20–80	181.5 ppm/°C	0.158
Ghanam et al. [6]	25–220	< –0.0005% FS/K	–
Shielded capacitive sensor [7]	–	Excellent thermal stability	–
Concave well DTMCPS [8]	–	Not reported	High (touch mode)
Analytical square diaphragm [9]	–	–	–
Material comparison for automotive [10]	25–100	Drift analyzed	–
Si-polysilicon sensor [11]	290–300 K	–	30×10^{-6} pF/Pa
Intraocular MEMS sensor [12]	–	–	–
Neural network compensation [13]	–	±0.5 hPa residual	–
In-sensor NN system [14]	–	±0.5 hPa residual	–
This work (with compensation)	0–260	28.52 ppm/°C	27.46
This work (without compensation)	0–220	7781 ppm/°C	18.8

Fig. 7 shows how the capacitance changes versus temperature for the compensated sensor (with spring K) under a pressure of 1000 Pa. Over the entire temperature range from 0 to 260 °C, the capacitance varies little and remains nearly constant, with an overall shift of less than 0.35 fF. The corresponding TCS is as small as 28.52 ppm/°C. Zero thermal drift proves that the suggested compensation geometry successfully compensates for the temperature dependence of Young's modulus.

Fig. 8 provides a similar analysis of the uncompensated sensor (without spring K). In contrast, there is a sharp increase in capacitance with temperature, ranging from ≈18.2 fF at 20 °C to ≈21.5 fF at 140 °C, with a total change of 3.3 fF. Such an increase is attributed solely to the temperature-dependent Young's modulus, resulting in excessive diaphragm deformation. Correspondingly, the TCS is estimated at 7781 ppm/°C, i.e., more than 270 times larger than the compensated sensor. From the foregoing analysis, one can see that the proposed two-spring structure achieves perfect thermal self-compensation without any electronics or post-processing.

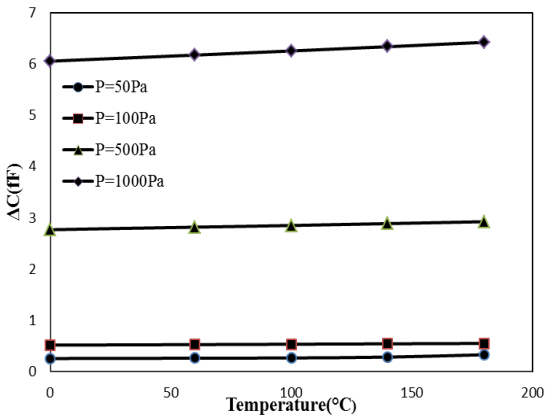

Fig. 7. Capacitance variation with temperature at constant pressure with spring K applied.

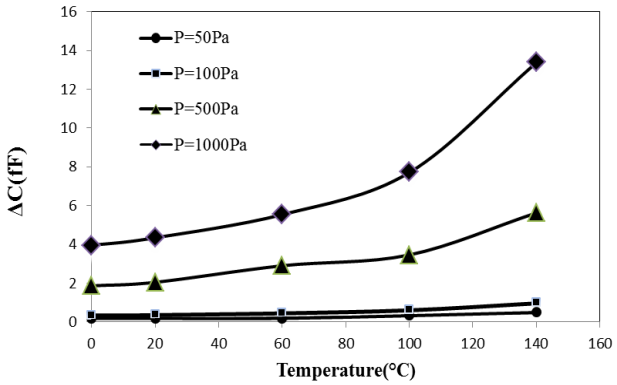

Fig. 8. Capacitance variation with temperature at constant pressure without spring K applied.

4 | Conclusion

In this study, we propose a novel geometrically self-compensated MEMS capacitive pressure sensor for temperature-drift-free Young's modulus compensation using a simple spring mechanism without electronic circuitry or post-fabrication calibration. The critical idea behind the design is the use of a double-spring system, with one spring (K) long and stiff, and the other (K') short and flexible. Differential thermal expansion creates a tensile force on the short spring, making it stiffer and offsetting the change in Young's modulus with temperature.

The effectiveness of this design was demonstrated using ANSYS finite element simulation. Results include:A maximum pressure measurement error of less than 33 Pa from 0 to 260 °C range, which shows a tenfold improvement over uncompensated sensors and is also better than many of the previous mechanical compensations. A TCS of 28.52 ppm/°C, which is the minimum TCS obtained using mechanical compensation alone without any electrical circuits.An extremely high sensitivity of 27.46 fF/kPa in a very small area of 0.03288 mm². A zero-power consumption for compensation, which is ideal for battery-powered and wireless sensors. Compared with the more recently developed neural network-based compensation techniques [13], [14] that achieve ±0.5 hPa error but require electronic circuitry and power consumption, the new sensing device provides comparable performance with the advantages of ease of operation, reliability, and no electrical overhead.

The future scope for research would include experimental evaluation of the device using its fabrication in a typical polysilicon surface micromachining technology, along with testing under varying temperature and

pressure conditions. The geometric compensation method may also be extended to other MEMS-based sensors sensitive to temperature changes, such as accelerometers, gyroscopes, and resonators.

Conflict of Interest

The authors declare no conflict of interest.

Data Availability

All data are included in the text.

Funding

This research received no specific grant from funding agencies in the public, commercial, or not-for-profit sectors.

References

[1] Damghanian, M., & Majlis, B. Y. (2009). Analysis and design of a wide micro beam as a pressure gauge for high sensitivity MEMS fingerprint sensors. *Microsystem technologies*, *15*(5), 731–737. https://doi.org/10.1007/s00542-008-0755-4

[2] Cong, P., Chaimanonart, N., Ko, W. H., & Young, D. J. (2009). A wireless and batteryless 10-bit implantable blood pressure sensing microsystem with adaptive RF powering for real-time laboratory mice monitoring. *IEEE journal of solid-state circuits*, *44*(12), 3631–3644. https://doi.org/10.1109/JSSC.2009.2035551

[3] Clausen, I., & Sveen, O. (2007). Die separation and packaging of a surface micromachined piezoresistive pressure sensor. *Sensors and actuators a: Physical*, *133*(2), 457–466. https://doi.org/10.1016/j.sna.2006.05.011

[4] Chang, S. P., & Allen, M. G. (2004). Demonstration for integrating capacitive pressure sensors with read-out circuitry on stainless steel substrate. *Sensors and actuators a: Physical*, *116*(2), 195–204. https://doi.org/10.1016/j.sna.2004.04.010

[5] Zhang, Y., Howver, R., Gogoi, B., & Yazdi, N. (2011). A high-sensitive ultra-thin MEMS capacitive pressure sensor. *2011 16th international solid-state sensors, actuators and microsystems conference* (pp. 112–115). IEEE. https://doi.org/10.1109/TRANSDUCERS.2011.5969151

[6] Ghanam, M., Bilger, T., Goldschmidtboeing, F., & Woias, P. (2022). *M*EMS self-packaged capacitive absolute pressure and force sensors for high-temperature applicatio. *2022 IEEE sensors* (pp. 1–4). IEEE. https://doi.org/10.1109/SENSORS52175.2022.9967300

[7] Ghanam, M., Goldschmidtboeing, F., Bilger, T., Bucherer, A., & Woias, P. (2023). MEMS shielded capacitive pressure and force sensors with excellent thermal stability and high operating temperature. *Sensors*, *23*(9), 4248. https://doi.org/10.3390/s23094248

[8] Kumar, G. A. A. U., Jindal, S. K., & P K, S. (2022). Capacitance response of concave well substrate MEMS double touch mode capacitive pressure sensor: Robust design, theoretical modeling, numerical simulation and performance comparison. *Silicon*, *14*(15), 9659–9667. https://doi.org/10.1007/s12633-022-01693-9

[9] Jindal, S. K., Patel, I., Sethi, K., Kaul, S., Sreekanth, P. K., & Kumar, A. (2022). Efficient in-depth analysis and optimum design parameter estimation of MEMS capacitive pressure sensor utilizing analytical approach for square diaphragm. *Journal of computational electronics*, *21*(4), 992–1004. https://doi.org/10.1007/s10825-022-01896-8

[10] Suman, S., Punetha, D., & Pandey, S. K. (2021). Improvement in sensing characteristics of silicon microstructure based MEMS capacitive sensor for automotive applications. *Silicon*, *13*(5), 1475–1483. https://doi.org/10.1007/s12633-020-00540-z

[11] Kehileche, B., Khoudrane, Y., Belmessaoud, B., Henini, N., & Chiba, Y. (2022). Performance analysis and enhancement of mems pressure sensor's sensitivity based on new materials. *Artificial intelligence and*

heuristics for smart energy efficiency in smart cities (pp. 779–785). Cham: Springer International Publishing. https://doi.org/10.1007/978-3-030-92038-8_79

[12] Mohd Noor, A., Zakaria, Z., & Saad, N. (2021). Intraocular mems capacitive pressure sensor. *Intelligent manufacturing and mechatronics* (pp. 493–501). Singapore: Springer Singapore. https://doi.org/10.1007/978-981-16-0866-7_42

[13] Licciardo, G. D., Vitolo, P., Bosco, S., Pennino, S., Pau, D., Pesaturo, M., … & Liguori, R. (2023). Ultra-tiny neural network for compensation of post-soldering thermal drift in mems pressure sensors. *2023 IEEE international symposium on circuits and systems (ISCAS)* (pp. 1–5). IEEE. https://doi.org/10.1109/ISCAS46773.2023.10181480

[14] Vitolo, P., Licciardo, G. D., Liguori, R., Di Benedetto, L., Rubino, A., Pau, D., & Pesaturo, M. (2024). In-sensor system for real-time compensation of thermal drift in mems pressure sensors. *Proceedings of sie 2023* (pp. 186–191). Cham: Springer Nature Switzerland. https://doi.org/10.1007/978-3-031-48711-8_21

[15] Thiem, C. D., & Hertline, J. M. (2009). Simulation concept-how to exploit tools for computing hybrids. https://apps.dtic.mil/sti/html/tr/ADA503259/

[16] Mastrangelo, C. H., Zhang, X., & Tang, W. C. (1996). Surface-micromachined capacitive differential pressure sensor with lithographically defined silicon diaphragm. *Journal of microelectromechanical systems*, *5*(2), 98–105. https://doi.org/10.1109/84.506197

[17] Ganji, B. A., & Shahiri-Tabarestani, M. (2013). A novel high sensitive MEMS intraocular capacitive pressure sensor. *Microsystem technologies*, *19*(2), 187–194. https://doi.org/10.1007/s00542-012-1688-5

[18] Hao, X. C., Jiang, Y. G., Takao, H., Maenaka, K., Fujita, T., & Higuchi, K. (2011). Zero temperature coefficient gas-sealed pressure sensor using mechanical temperature compensation. *2011 16th international solid-state sensors, actuators and microsystems conference* (pp. 116–119). IEEE. https://doi.org/10.1109/TRANSDUCERS.2011.5969152

[19] Eswaran, P., & Malarvizhi, S. (2012). Sensitivity analysis on mems capacitive differential pressure sensor with bossed diaphragm membrane. *2012 international conference on devices, circuits and systems (ICDCS)* (pp. 704–707). IEEE. https://doi.org/10.1109/ICDCSyst.2012.6188688

[20] He, F., Huang, Q. A., & Qin, M. (2007). A silicon directly bonded capacitive absolute pressure sensor. *Sensors and actuators a: Physical*, *135*(2), 507–514. https://doi.org/10.1016/j.sna.2006.09.022